

# Attitude Control Thruster Plume Flow Modeling and Experiments

G. Dettleff,\* R.-D. Boettcher,\* C. Dankert,\* G. Koppenwallner,†  
and H. Legge‡

*DFVLR Institute for Experimental Fluid Mechanics, Göttingen, Federal Republic of Germany*

A plume flow model has been developed to calculate the impingement forces and heat transfer caused by the firing of attitude control thrusters on satellites. Its validity for the inviscid core flow was tested and verified by an experimental study including pitot pressure and velocity measurements in plumes with different pure test gases. Measurements in real hydrazine thruster plumes allowed the determination of essential data (especially an effective ratio of specific heats) necessary for the description of this flowfield.

## Nomenclature

$A_E$	= cross section of nozzle exit
$A_P, A_{P,mod}$	= plume constant <sup>1</sup>
$A_{P,exp}$	= plume constant, determined by experiment
$b$	= factor of proportionality in Eq. (12)
$c_p, c_v$	= specific heats at constant pressure and volume, respectively
$dA$	= surface element
$d_p$	= diameter of pitot probe
$l_E$	= distance from nozzle throat to nozzle exit
$\dot{m}$	= mass flow
$M$	= molecular mass
$Ma$	= Mach number
$\mathbf{n}$	= surface normal vector
$p_0$	= stagnation pressure
$p_{t2}$	= pitot pressure
$p_{t2,cl}$	= pitot pressure on centerline
$R$	= (specific) gas constant
$Re_E$	= nozzle Reynolds number, $Re_E = \rho_E \cdot u_E \cdot l_E / \mu(T_0)$
$r$	= radius, polar coordinate
$r^*$	= nozzle throat radius
$r_E$	= nozzle exit radius
$T_0$	= stagnation temperature
$u$	= velocity
$u^*$	= velocity at nozzle throat
$u_E$	= velocity at nozzle exit (isentropic flow)
$u_{exp}$	= velocity determined by experiment
$u_{lim}$	= maximum gas velocity $\sqrt{2k/(\kappa-1) \cdot R \cdot T_0}$
$x_0$	= virtual source point of streamlines
$x, y$	= coordinates
$y_b$	= plume boundary coordinate
$\delta_E$	= boundary-layer thickness at nozzle exit
$\theta$	= angle, polar coordinate
$\theta_0$	= angle between plume axis and streamline, which separates the isentropic core and the boundary-layer expansion region
$\theta_{lim}$	= maximum expansion angle
$\theta_n$	= angle between surface normal and streamline (Fig. 9)
$\kappa$	= ratio of specific heats
$\mu$	= viscosity

$\pi$	= 3.14...
$\rho$	= density
$\rho_E$	= density at nozzle exit
$\rho_0$	= density in stagnation chamber
$\rho^*$	= density at nozzle throat
<i>Subscript</i>	
hy	= hydrazine plume

## Introduction

TO determine the plume flow and impingement effects caused by the firing of attitude control thrusters on satellites, an extensive study is being performed at the DFVLR Institute for Experimental Fluid Mechanics. In the recent years, a model has been developed and implemented as a computer code to determine all of the relevant flow quantities as well as forces and heat transfer due to impingement. A complete description of the model has been presented by Boettcher, Legge, and their colleagues.<sup>1,2</sup>

In an experimental study, pure test gases were used to verify the model description and to test the influence of various parameters on the plume flow behavior. Moreover, experiments were performed in hydrazine thruster plumes to obtain input data for the model calculation and to demonstrate its applicability to the realistic case.

In this paper, we present essential features of the model with respect to impingement problems and we report on experiments to verify the model description of the density and velocity in the inviscid continuum regime of the plume.

## Model

Basic ideas of the model for the continuum flowfield have been adopted from Simons<sup>3</sup> and Boynton.<sup>4</sup> The plume flow is subdivided into the isentropic core and the boundary layer expansion region (Fig. 1). The edge of the boundary layer expansion region is defined by the angle  $\theta_0$ , which depends essentially on the nozzle boundary-layer thickness. The streamlines are straight lines with the origin in the center of the nozzle exit. For reasons of easy computation, the flow is cut off at the maximum expansion angle  $\theta_{lim}$ , which is obtained assuming a two-dimensional Prandtl-Meyer expansion at the nozzle lip.

Continuum as well as transition and free molecular flow are treated in the model. The latter are, however, not subject of this paper.

The density  $\rho$  and the gas velocity  $u$  are the most important flow quantities with respect to impingement effects. Their careful determination is indispensable when dealing with impingement problems. In this paper, the model description of

Presented as Paper 85-0933 at the AIAA 20th Thermophysics Conference, Williamsburg, VA, June 19-21, 1985; revision submitted Dec. 16, 1985. Copyright © American Institute of Aeronautics and Astronautics, Inc., 1985. All rights reserved.

\*Research Scientist.

†Section Head, Member AIAA.

‡Research Scientist, Member AIAA.

these two quantities and their experimental determination in the expansion flow of the isentropic core are presented.

In the continuum flow regime the density  $\rho(r, \theta)$  is given by<sup>3</sup>

$$\rho/\rho^* = A_{P, \text{mod}} \cdot (r^*/r)^2 \cdot f(\theta) \quad (1)$$

with

$$f(\theta) = \cos^{2/(\kappa-1)} \left( \frac{\pi \cdot \theta}{2 \cdot \theta_{\text{lim}}} \right) \quad (2)$$

the density distribution function for the isentropic core  $0 \leq \theta \leq \theta_0$  (Fig. 1), and

$$\frac{A_P = u^*/(2 \cdot u_{\text{lim}})}{\int_0^{\theta_{\text{lim}}} f(\theta) \cdot \sin \theta \cdot d\theta} \quad (3)$$

Equation (3) is derived from the continuity equation relating the nozzle flow at the throat to the plume flow in the far field where  $u = u_{\text{lim}}$ . The angle  $\theta_0$  and, therefore, the integral in Eq. (3), depends on the nozzle boundary-layer thickness<sup>1</sup>

$$\delta_E = 6.25 / \sqrt{Re_E} \cdot l_E \quad (4)$$

with the nozzle Reynolds number

$$Re_E = \rho_E \cdot u_E \cdot l_E / \mu(T_0) \quad (5)$$

Therefore, for fixed nozzle geometry, the plume constant  $A_P$  depends on  $Re_E$  and  $\kappa$ , the ratio of specific heats,

$$A_P = A_P(Re_E, \kappa) \quad (6)$$

Knowing  $\rho$  and the stagnation conditions, the gas velocity  $u$  in the isentropic core can be calculated by means of the equations for a perfect-gas flow.<sup>5</sup>

### Experiments

The experiments have been carried out in the third test section of the DFVLR vacuum wind tunnel in Göttingen (using pure test gases) and with real hydrazine thrusters at the facilities of the German aerospace company MBB/ERNO. The setup and the nozzles are sketched in Fig. 2.

For the tests with pure gases the stagnation pressure  $p_0$  could be varied up to 16 bar and a heater allowed to attain stagnation temperatures  $T_0$  up to 800 K. Both quantities were adjusted to simulate realistic nozzle Reynolds numbers [Eq. (5)] as for hydrazine thrusters.

Typical mass flow rates are of the order of 1 g/s. Roots blowers with a pumping capability of 30 m<sup>3</sup>/s provided a vacuum chamber pressure of typically 0.01–0.05 mbar. Due to this background pressure, only a limited gas expansion is possible. The unavoidable barrel shock system (Fig. 2) restricts our measurements in this study to the isentropic core region and did not allow an investigation of the boundary-layer expansion region.

The gas velocity  $u$  was measured directly with an "ion time of flight" technique using an electron beam of about 18 keV. Molecules of the expanding plume gas are ionized and detected further downstream with a tungsten wire probe. Shifting the probe by  $\Delta r$  and measuring the corresponding flight time  $\Delta t$  directly delivers the velocity  $u = \Delta r / \Delta t$  along a streamline.

When the gas velocity and the ratio of specific heats are known the density can be determined by means of pitot pressure measurements. In the hypersonic plume flow, the pitot pressure  $p_{i2}$  can be approximated by

$$p_{i2} = \frac{\kappa + 3}{\kappa + 1} \cdot \frac{1}{2} \cdot \rho \cdot u^2 \quad (7)$$

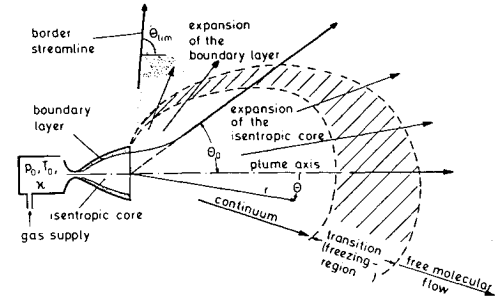


Fig. 1 Flow regions in plume.

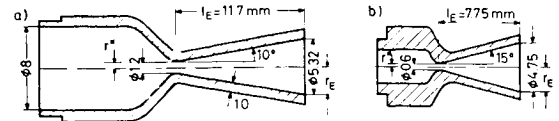
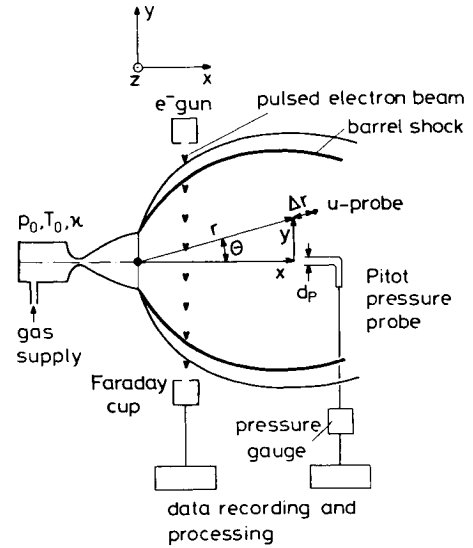


Fig. 2 Experimental setup for gas velocity and pitot pressure measurements. Nozzles: a) 10 deg conical nozzle, b) MBB/ERNO 0.5 N hydrazine thrust nozzle (15 deg).

For the measurements of  $p_{i2}$ , we use probes with diameters  $d_p = 2, 6$ , and 20 mm depending on the rarefaction of the flow. A traversing mechanism allowed the probes to move along the axis and perpendicular to it. For the model testing, especially of Eq. (1), we used the pure gases  $\text{CF}_4$ ,  $\text{N}_2$ , and Ar. These gases cover a large range of the most sensitive parameter  $\kappa$  (ratio of specific heats). Moreover pitot pressure measurements were performed in the plume of the MBB/ERNO 0.5 N monopropellant hydrazine thruster to obtain input data for the model calculation.

### Results

#### Experiments with Pure Gases

The gas velocity has been measured in plumes emanating from the 10 deg conical nozzle (Fig. 2). The results of the measurements in the region  $x/r_E > 20$  ( $r_E$  is the nozzle exit radius) are listed in Table 1. Here the velocity has been found to be constant everywhere on the plume axis at fixed stagnation conditions. The comparison of  $u_{\text{exp}}$  and

$$u_{\text{lim}} = \sqrt{\frac{2\kappa}{(\kappa-1)} \cdot R \cdot T_0} \quad (8)$$

**Table 1** Velocity measurements on the plume axis  
( $x/r_E > 20$ , 10 deg conical nozzle)

Gas	$\kappa$	$p_0$ , bar	$T_0$ , K	$u_{exp}$ , m/s	$u_{lim}$ , m/s	$\frac{u_{exp}}{u_{lim}}$
N <sub>2</sub>	1.4	1.25	294	772	781	0.99
		4.0	295	759	782	0.97
		8.0	290	794	776	1.02
CF <sub>4</sub>	1.14	1.25	821	1117	1123	0.99
N <sub>2</sub>	1.4	3.25	812	1304	1298	1.00
AR	1.67	3.25	813	980	917	1.07

shows that we have realized the maximum gas velocity  $u_{lim}$  for a perfect gas. Therefore, we can define the region  $x/r_E > 20$  as the far field with  $u \approx u_{lim}$  and practically straight streamlines.

This result is in agreement with the model, where the velocity  $u$  in the isentropic core is described by

$$u = \sqrt{\frac{2\kappa \cdot R \cdot T_0}{(\kappa - 1) + 2/Ma^2}} \quad (9)$$

For  $x/r_E \geq 20$  we find in the plumes behind the 10 deg nozzle  $Ma > 10$ . In this case  $\kappa - 1 \gg 2/Ma^2$  in Eq. (9), so that Eqs. (9) and (8) become practically identical. The difference is smaller than 5%.

The variation of the nozzle Reynolds number by means of the variation of the stagnation pressure  $p_0$  with N<sub>2</sub> as test gas shows no particular influence of  $Re_E$  on  $u_{exp}$  for  $5 \times 10^2 < Re_E < 2 \times 10^4$ .

For the pitot pressure measurements we used the 15 deg conical nozzle (nozzle of the MBB/ERNO 0.5 N hydrazine thruster). In Fig. 3, we show two axial pitot pressure profiles measured in plumes with N<sub>2</sub> as test gas. The different stagnation pressures  $p_0$  correspond to different nozzle Reynolds numbers  $Re_E$ .

For  $x/r_E > 20$  we are in the far field, i.e., the maximum gas velocity  $u_{lim}$  is reached. Then we can approximate the pitot

pressure  $p_{t2}$  by

$$p_{t2} = \frac{\kappa + 3}{\kappa + 1} \cdot \frac{1}{2} \cdot \rho \cdot u_{lim}^2 \quad (10)$$

For the density along a streamline, we obtain

$$\rho \sim 1/(x - x_0)^2 \quad (11)$$

with  $x_0$  as virtual source point position of the streamlines. The combination of Eqs. (10) and (11) yields (with proper scaling factors),

$$\frac{p_{t2}}{p_0} = b \cdot \frac{r^{*2}}{(x - x_0)^2} \quad (12)$$

Since  $p_{t2}$ ,  $p_0$ ,  $x$ , and  $r^*$  are measured, we can determine  $x_0$  and the factor of proportionality  $b$  by a best fit approximation.

The values of  $b$  and  $x_0$  for three axial profiles are listed in Fig. 3. We consider  $b$  as the essential quantity describing the pitot pressure distribution along the plume axis. The virtual source point positions  $x_0$  differ only slightly from the model value  $x_0 = 0$ .

Using Eqs. (8), (10), the ideal-gas equation

$$p_0 = \rho_0 \cdot R \cdot T_0 \quad (13)$$

and

$$\frac{\rho^*}{\rho_0} = \left(1 + \frac{\kappa - 1}{2}\right)^{-1/(\kappa - 1)} \quad (14)$$

with Eq. (12), we get

$$\frac{\rho}{\rho^*} = A_{p,exp} \cdot \frac{r^{*2}}{(x - x_0)^2} \quad (15)$$

with

$$A_{p,exp} = b \cdot \frac{1}{f(\kappa)} \quad (16)$$

$$f(\kappa) = \frac{\kappa + 3}{\kappa + 1} \cdot \frac{\kappa}{\kappa - 1} \cdot \left(1 + \frac{\kappa - 1}{2}\right)^{-1(\kappa - 1)} \quad (17)$$

Comparing Eqs. (1) and (15) we find that  $A_p$ , which describes the density along the plume axis, can be determined by means of  $b$ , obtained from the measured axial pitot pressure profiles, and a known function  $f(\kappa)$  [for  $\theta = 0$ ,  $f(\theta) = 1$  in Eqs. (1) and (2)].

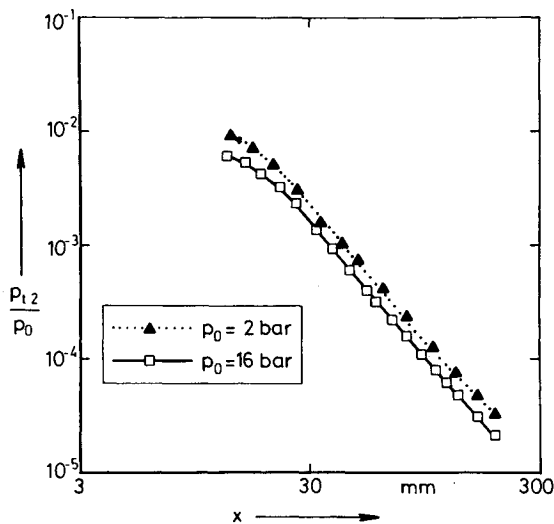
When the nozzle geometry is fixed, we have for equilibrium flow

$$A_p = A_p(Re_E, \kappa) \quad (18)$$

In the following we investigate  $A_p(Re_E)$  for constant  $\kappa$  and  $A_p(\kappa)$  for fixed  $Re_E$ .

In Fig. 4  $A_p$  is plotted vs  $Re_E$ . The test gas is N<sub>2</sub> (constant  $\kappa$ ). The results for  $T_0 = 300$  K have been obtained from profiles as shown in Fig. 3. Larger values of  $A_{p,exp}$  have been obtained for the elevated stagnation temperature  $T_0 = 800$  K. The result  $A_{p,mod} = f(Re_E)$  of the model calculation is qualitatively correct. The deviations between  $A_{p,mod}$  and  $A_{p,exp}$  exceed in only one case 15%. Nevertheless, it seems to be necessary to introduce the dependence  $A_p(T_0)$  for fixed  $Re_E$  and a possible nozzle wall temperature influence into the model.

In a second experimental series,  $A_p$  was investigated as function of  $\kappa$  (Fig. 5). With respect to the foregoing results, the Reynolds number  $Re_E$  was kept constant in the experiments. This was achieved by proper adjustment of  $p_0$  at a constant stagnation temperature of  $T_0 = 800$  K. CF<sub>4</sub> ( $\kappa = 1.14$ ),



$p_0$ , bar	$b$	$x_0$ , mm	$x_0/r_E$	$Re_E$
2	12.1	9	3.8	3300
16	8	11	4.6	26000

**Fig. 3** Axial pitot pressure profiles (nozzle MBB/ERNO 0.5 N, test gas N<sub>2</sub>,  $T_0 = 300$  K, parameter  $p_0$ ). Approximation  $p_{t2}/p_0 = b \cdot (r^{*2}/(x - x_0)^2)$ ,  $x/r_E > 20$ .

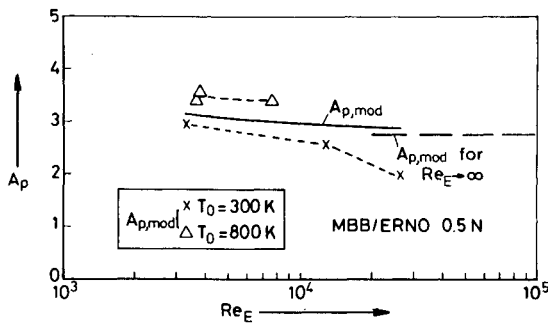


Fig. 4  $A_P$  as a function of  $Re_E$  (MBB/ERNO 0.5 N nozzle, test gas  $N_2$ ).

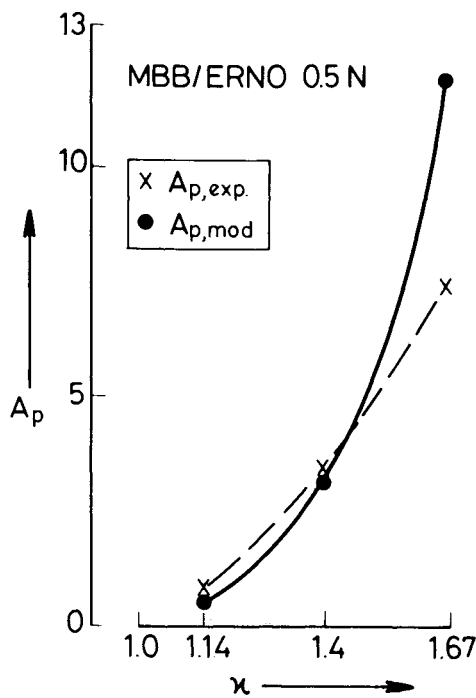


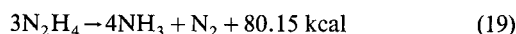
Fig. 5  $A_P$  as a function of  $\kappa$  (MBB/ERNO 0.5 N nozzle, three different test gases,  $T_0 = 800$  K,  $Re_E = 3600$ ).

$N_2$  ( $\kappa = 1.4$ ), and Ar ( $\kappa = 1.67$ ) were used as the test gases. The deviations between the model and experimental results are acceptable for  $\kappa < 1.4$ ; however, the deviations are larger for Ar. In the corresponding velocity measurements, we have found  $u_{exp} > u_{lim}$  in argon plumes, which might indicate condensation in the expansion flow.

#### Experiments with Hydrazine Thruster Plumes

Pitot pressure measurements were also performed in hydrazine thruster plumes (MBB/ERNO 0.5 N thruster, Fig. 2). By means of the evaluation of the axial profiles, we obtained  $b$  as in the experiments with pure test gases by assuming  $u \approx u_{lim}$  for  $x/r_E > 20$ . The determination of  $A_{P,exp} = b/f(\kappa)$ , however, requires the determination of the (unknown) ratio of specific heats  $\kappa$ , which is the most sensitive parameter in the model description.

Hydrazine ( $N_2H_4$ ) is decomposed according to the following main reactions<sup>6</sup>:



The composition of the gas in the combustion chamber, its ratio of specific heats, and its temperature  $T_0$  depend essen-

tially on the unknown dissociation degree of  $NH_3$ . If the first reaction alone takes place, then  $T_0 = 1649$  K. If  $NH_3$  is decomposed completely,  $T_0 = 867$  K.

By means of the results of the pitot pressure measurements, it was possible to determine an effective ratio of specific heats for the hydrazine plumes. The objective is to interpolate  $\kappa_{hy}$  for the MBB/ERNO 0.5 N hydrazine thruster plume by means of  $b_{hy}$  obtained from the axis pitot pressure profiles.

In Fig. 6  $b$  is shown as function of  $\kappa$ , obtained from experiments with the 15 deg conical nozzle (MBB/ERNO 0.5 N thruster nozzle, Fig. 2) using different test gases. These experiments have been described in the foregoing section.

The value of  $b_{hy}$  for  $Re_E = 3600$  has been interpolated from the curve of  $b_{hy} = f(Re_E)$  in Fig. 7. For each value of  $p_0$ , only a certain range of  $Re_E$  could be determined, since the viscosity  $\mu(T_0)$  in Eq. (5) depends on the dissociation of  $NH_3$  [Eq. (20)]. We have calculated  $\mu(T_0)$  for complete dissociation with  $T_0 = 867$  K and for the case of no dissociation with  $T_0 = 1649$  K. The corresponding range of  $Re_E$  is indicated by the horizontal bar for each value of  $p_0$ . For  $Re_E = 3600$  we obtain  $b_{hy} = 13$  and, by means of this value, we interpolate  $\kappa_{hy} = 1.37$  in Fig. 6.

We consider  $\kappa_y = 1.37$  for the exhaust gas as an effective ratio of specific heats. This value has been derived from the

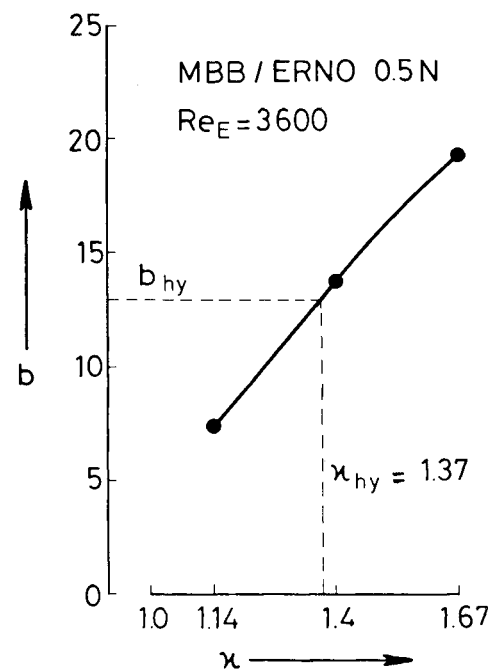


Fig. 6  $b$  as a function of  $\kappa$  (MBB/ERNO 0.5 N nozzle, three different test gases,  $T_0 = 800$  K,  $Re_E = 3600$ , interpolation of  $\kappa_{hy}$  by means of  $b_{hy}$  from Fig. 7).

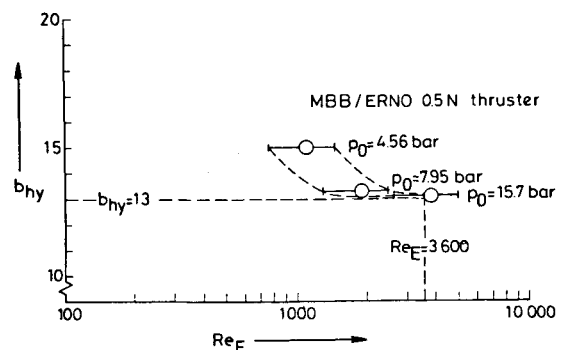


Fig. 7  $b_{hy}$  as a function of  $Re_E$  (MBB/ERNO 0.5 N hydrazine thruster). Bars correspond to the possible range of  $Re_E$  for fixed  $p_0$ .

gas expansion behavior and not from a measurement of the specific heats  $c_p$  and  $c_v$ .

The ratio of specific heats influences the shape of the transverse profiles  $\rho(\theta)$  for fixed  $r$  according to Eq. (2) for the function  $f(\theta)$ . Figure 8 compares two normalized transverse pitot pressure profiles that were obtained from the experiments and from a model calculation with  $\kappa = 1.37$ . In the far field, it is  $p_{t2} \sim \rho$  and

$$p_{t2}(y) \sim f(y) \cdot \cos^{2/(\kappa-1)} \left( \frac{\pi}{2} \cdot \frac{\theta}{\theta_{\text{lim}}} \right) \quad (21)$$

for a fixed coordinate  $x$  [ $f(y)$  is a simple geometric function]. The agreement between the two normalized profiles is good, thus confirming the validity of  $f(\theta)$  in the isentropic core with  $\kappa = 1.37$ .

To apply Eqs. (12) and (21) to the evaluation of pitot pressure profiles, the gas velocity must have reached its maximum. Due to safety requirements, we could not use the time-of-flight method (18 kV d.c.) for the measurement of  $u_{\text{exp}}$  in the MBB/ERNO facilities during the thruster firing. Nevertheless, a mean gas velocity can be estimated by the evaluation of transverse pitot pressure profiles. Rewriting Eq. (7) yields

$$\rho \cdot u = 2 \cdot \frac{\kappa + 1}{\kappa + 3} \cdot p_{t2} \cdot \frac{1}{u} \quad (22)$$

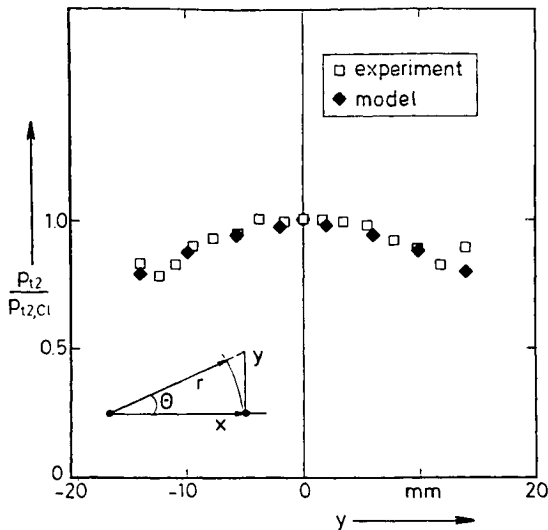


Fig. 8 Normalized pitot pressure profiles  $p_{t2}/p_{t2,cl}$  as function of  $y$  (MBB/ERNO 0.5 N hydrazine thruster,  $p_0 = 15.7$  bar,  $x/r_E = 32$ ).

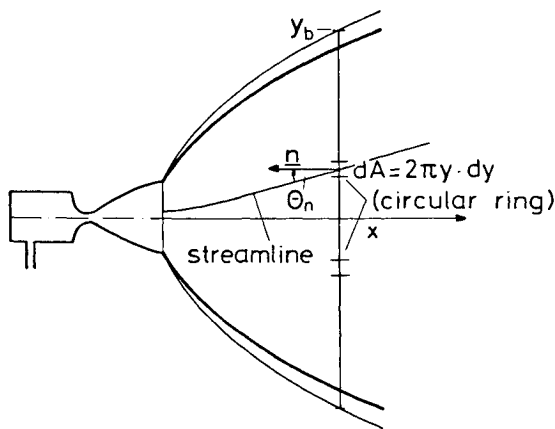


Fig. 9 Plume cross section with surface element  $dA$  and plume border  $y_b$ .

By integration over the whole plume cross section (Fig. 9), we obtain the total mass flow,

$$\int_{\text{plume cross section}} \rho \cdot u \cdot \cos \theta_n \cdot dA = \dot{m} = 2 \cdot \frac{\kappa + 1}{\kappa + 3} \int_{\text{plume cross section}} \frac{1}{u} \cdot p_{t2} \cdot \cos \theta_n \cdot dA \quad (23)$$

Using  $\cos \theta_n \approx 1$ , i.e., assuming that the angle between the streamlines and the surface normal  $n$  is small (actually  $\theta_n < 25$  deg at  $y_b$ , Fig. 2), and regarding  $u$  as the mean velocity over the plume cross section,  $u$  can be taken in front of the integral in Eq. (23)

$$u \approx \frac{2}{\dot{m}} \cdot \frac{\kappa + 1}{\kappa + 3} \int_{\text{plume cross section}} p_{t2} \cdot dA \quad (24)$$

The evaluation of two transverse pitot pressure profiles, measured at  $x/r_E = 8$  and 16 yields for  $Re_E \approx 3600$

$$u \approx 2300 \dots 2600 \text{ m/s}$$

This result can also be obtained by Eq. (8),

$$u_{\text{lim}} = \sqrt{\frac{2\kappa}{\kappa - 1} \cdot R \cdot T_0} \approx 2400 \text{ m/s}$$

if we use  $\kappa_{hy} = 1.37$  (determined previously),  $R \approx 638 \text{ J/kg} \cdot \text{K}$ , and  $T_0 \approx 1200 \text{ K}$  deduced from heat transfer measurements in the same hydrazine thruster plume<sup>7</sup> for  $Re_E \approx 3600$ . Similar results for the gas velocity are obtained in a more accurate estimate.<sup>7</sup>

## Conclusions

To verify an existing plume flow model an experimental study is under way at the DFVLR in Göttingen. In this paper, we have reported on a study of the density and velocity distribution in the isentropic core. Different pure test gases and conical nozzles were used. Parameters were the nozzle Reynolds number and the ratio of specific heats.

The far-field assumption of the model was verified. This means that the maximum gas velocity is reached and that the streamlines are straight except for a small region immediately downstream of the nozzle. Their virtual source is in the vicinity of the exit.

The density distribution along the plume axis was verified for different gases and nozzle Reynolds numbers. Both the density and velocity are of particular interest, since they essentially determine the impingement effects due to the thruster firing. The experimental results for the relation between the density and Reynolds number show that the stagnation and nozzle wall temperature should be introduced into the model as parameters.

Measurements in hydrazine thruster plumes allowed the determination of an effective ratio of specific heats for the exhaust gas with unknown composition. The value  $\kappa_{hy} = 1.37$  of this most sensitive parameter of the plume flow has been obtained from the gas expansion behavior and is therefore called effective.

The gas velocity in hydrazine thruster plumes was estimated by the evaluation of pitot pressure measurements. The results are in agreement with a calculation using the equation for the maximum gas velocity.

The results of this study verify the model description for the two essential flow quantities (with respect to impingement problems)  $\rho$  and  $u$  in the isentropic core flow. It is remarkable that the perfect-gas equations with constant gas properties (especially  $\kappa = \text{const}$ ) can be applied though chemical reactions and freezing of molecular degrees of freedom are likely to take place at least in the nozzle.

### Acknowledgment

This work was supported by the European Space Agency (ESA) through Contract ESTEC 5194/82/NL/PB(SC).

### References

<sup>1</sup>Legge, H. and Boettcher, R.-D., "Modelling Control Thruster Plume Flow and Impingement," *Proceedings of the 13th International Symposium on Rarefied Gas Dynamics*, Novosibirsk/USSR, 1982.

<sup>2</sup>Boettcher, R.-D., Dettleff, G., Koppenwallner, G., and Legge, H., "A Study of Rocket Exhaust Plumes and Impingement Effects on Spacecraft Surfaces," European Space Agency, Paris, Rept. CR(P)-1698, 1982.

<sup>3</sup>Simons, G.A., "Effect of Nozzle Boundary Layers on Rocket Exhaust Plumes," *AIAA Journal*, Vol. 10, Nov. 1972, pp. 1534-1535.

<sup>4</sup>Boynton, F.P., "Highly Underexpanded Jet Structure. Exact and Approximate Calculations," *AIAA Journal*, Vol. 5, Sept. 1967, pp. 1703-1705.

<sup>5</sup>"Equation, Tables, and Charts for Compressible Flow," NACA Rept. 1135, 1953.

<sup>6</sup>Lewis, B., Pease, R.N., and Taylor, H.S. (editors), "High Speed Aerodynamics and Jet Propulsion," *Combustion Process*, Vol. 11, Princeton University Press, Princeton, NJ, 1956.

<sup>7</sup>Legge, H. and Dettleff, G., "Pitot Pressure and Heat Transfer Measurements in Hydrazine Thruster Plumes," AIAA Paper 85-0934, 1985.

*From the AIAA Progress in Astronautics and Aeronautics Series...*

## ENTRY VEHICLE HEATING AND THERMAL PROTECTION SYSTEMS: SPACE SHUTTLE, SOLAR STARPROBE, JUPITER GALILEO PROBE—v. 85

## SPACECRAFT THERMAL CONTROL, DESIGN, AND OPERATION—v. 86

*Edited by Paul E. Bauer, McDonnell Douglas Astronautics Company  
and Howard E. Collicott, The Boeing Company*

The thermal management of a spacecraft or high-speed atmospheric entry vehicle—including communications satellites, planetary probes, high-speed aircraft, etc.—within the tight limits of volume and weight allowed in such vehicles, calls for advanced knowledge of heat transfer under unusual conditions and for clever design solutions from a thermal standpoint. These requirements drive the development engineer ever more deeply into areas of physical science not ordinarily considered a part of conventional heat-transfer engineering. This emphasis on physical science has given rise to the name, thermophysics, to describe this engineering field. Included in the two volumes are such topics as thermal radiation from various kinds of surfaces, conduction of heat in complex materials, heating due to high-speed compressible boundary layers, the detailed behavior of solid contact interfaces from a heat-transfer standpoint, and many other unconventional topics. These volumes are recommended not only to the practicing heat-transfer engineer but to the physical scientist who might be concerned with the basic properties of gases and materials.

*Volume 85—Published in 1983, 556 pp., 6 × 9, illus., \$35.00 Mem., \$55.00 List  
Volume 86—Published in 1983, 345 pp., 6 × 9, illus., \$35.00 Mem., \$55.00 List*

TO ORDER WRITE: Publications Order Dept., AIAA, 1633 Broadway, New York, N.Y. 10019